whereas SAF32 strongly inhibited the generation/accumulation of PrP^{Sc}. Similar results have been reported in which a PrP^{Sc}-specific antibody had no prion-clearing effect, whereas the PrP^{C}-specific antibody showed marked clearing activity (10). Because the mimotope of PRB7 is located at 128–132, if this β-pleated sheet forms an interface for prion aggregation PRB7 IgG may block the assembly of PrP aggregates because the binding IgG is much larger than the target molecule (PrP). We examined this activity using FF32 cells or N2aL1 cells and obtained the same results as for ScN2a cells (data not shown). In this respect, our result suggested that, in the prion conversion reaction, PRB7 IgG-recognizing β-form PrP did not play a role in driving the conversion of the PrP conformation and appears rather to be an end product that loses prion activity and accumulates in the cytoplasm. This end product may trigger cell cytotoxicity via the mitochondrial machinery (42). This is in concert with the result that β-form recombinant PrP does not work as a template for prion amplification in protein misfolding cyclic amplification (41, 48). It is conceivable that PRB7-negative, SAF32-positive granules as a full-length, non-β-form PrP might be responsible for prion propagation (Fig. 10, *C* and *E*). Our results may be in agreement with the finding that prion propagation and toxicity *in vivo* occur in two distinct mechanistic phases (42). Thus, we have not obtained evidence to determine whether PRB7-recognizing β-form PrP represents the so-called PrP^{Sc} that has both conversion activity and cell cytotoxicity. Further investigation is needed to determine whether β-form PrP affinity-purified with PRB7 shows prion activity such as the infectious and conversion/accumulation activity of the prion.

Although a number of studies illuminated the accumulation of PrP^{res} in prion-infected cells or brain extracts, there is little literature giving much attention to the phenomenon in which most prion-infected ScN2a cells vigorously proliferate to survive in culture (49). The low frequency of PRB7 IgG-positive granules in ScN2a cells suggests the stochastic nature of the conversion of α-form to β-form PrP. The spongelike degeneration of prion-infected brain may reflect this feature.

In conclusion, we report the establishment of PRB7 IgG, which is the first human antibody discriminating the β-form from the α-form of PrP in the physiological condition. Using this antibody, we have demonstrated direct evidence of the generation and accumulation of β-form PrP in prion-infected ScN2a cells. It can be used to purify β-form PrP molecules without the need for protease digestion and may be useful to demonstrate the biochemical basis of the relationship of β-form PrP to PrP^{Sc} and to elucidate the structure-based evidence for prion infectivity and neurotoxicity.

Acknowledgments—We thank Mayumi Yamamoto and Yuko Sato for the initial study on this theme.

REFERENCES

1. Prusiner, S. B. (1998) Prions. *Proc. Natl. Acad. Sci. U.S.A.* **95,** 13363–13383
2. Rogers, M., Yehiely, F., Scott, M., and Prusiner, S. B. (1993) Conversion of truncated and elongated prion proteins into the scrapie isoform in cultured cells. *Proc. Natl. Acad. Sci. U.S.A.* **90,** 3182–3186
3. Pan, K. M., Baldwin, M., Nguyen, J., Gasset, M., Serban, A., Groth, D., Mehlhorn, I., Huang, Z., Fletterick, R. J., and Cohen, F. E.(1993) Conversion of α-helices into β-sheets features in the formation of the scrapie prion proteins. *Proc. Natl. Acad. Sci. U.S.A.* **90,** 10962–10966
4. Prusiner, S. B., McKinley, M. P., Bowman, K. A., Bolton, D. C., Bendheim, P. E., Groth, D. F., and Glenner, G. G. (1983) Scrapie prions aggregate to form amyloid-like birefringent rods. *Cell* **35,** 349–358
5. Turk, E., Teplow, D. B., Hood, L. E., and Prusiner, S. B. (1988) Purification and properties of the cellular and scrapie hamster prion proteins. *Eur. J. Biochem.* **176,** 21–30
6. Biasini, E., Tapella, L., Mantovani, S., Stravalaci, M., Gobbi, M., Harris, D. A., and Chiesa, R. (2009) Immunopurification of pathological prion protein aggregates. *PLoS One* **4,** e7816
7. Wadsworth, J. D., Joiner, S., Hill, A. F., Campbell, T. A., Desbruslais, M., Luthert, P. J., and Collinge, J. (2001) Tissue distribution of protease resistant prion protein in variant Creutzfeldt-Jakob disease using a highly sensitive immunoblotting assay. *Lancet* **358,** 171–180
8. Bocharova, O. V., Breydo, L., Parfenov, A. S., Salnikov, V. V., and Baskakov, I. V. (2005) *In vitro* conversion of full-length mammalian prion protein produces amyloid form with physical properties of PrP(Sc). *J. Mol. Biol.* **346,** 645–659
9. Khalili-Shirazi, A., Kaisar, M., Mallinson, G., Jones, S., Bhelt, D., Fraser, C., Clarke, A. R., Hawke, S. H., Jackson, G. S., and Collinge, J. (2007) β-PrP form of human prion protein stimulates production of monoclonal antibodies to epitope 91–110 that recognise native PrPSc. *Biochim. Biophys. Acta* **1774,** 1438–1450
10. Petsch, B., Müller-Schiffmann, A., Lehle, A., Zirdum, E., Prikulis, I., Kuhn, F., Raeber, A. J., Ironside, J. W., Korth, C., and Stitz, L. (2011) Biological effects and use of PrP^{Sc}- and PrP-specific antibodies generated by immunization with purified full-length native mouse prions. *J. Virol.* **85,** 4538–4546
11. Ishibashi, D., Yamanaka, H., Yamaguchi, N., Yoshikawa, D., Nakamura, R., Okimura, N., Yamaguchi, Y., Shigematsu, K., Katamine, S., and Sakaguchi, S. (2007) Immunization with recombinant bovine but not mouse prion protein delays the onset of disease in mice inoculated with a mouse-adapted prion. *Vaccine* **25,** 985–992
12. Jackson, G. S., Hosszu, L. L., Power, A., Hill, A. F., Kenney, J., Saibil, H., Craven, C. J., Waltho, J. P., Clarke, A. R., and Collinge, J. (1999) Reversible conversion of monomeric human prion protein between native and fibrilogenic conformations. *Science* **283,** 1935–1937
13. Hamasaki, T., Hashiguchi, S., Ito, Y., Kato, Z., Nakanishi, K., Nakashima, T., and Sugimura, K. (2005) Human anti-human IL-18 antibody recognizing the IL-18-binding site 3 with IL-18 signaling blocking activity. *J. Biochem.* **138,** 433–442
14. Tanaka, K., Nishimura, M., Yamaguchi, Y., Hashiguchi, S., Takiguchi, S., Yamaguchi, M., Tahara, H., Gotanda, T., Abe, R., Ito, Y., and Sugimura, K. (2011) A mimotope peptide of Aβ42 fibril-specific antibodies with Aβ42 fibrillation inhibitory activity induces anti-Aβ42 conformer antibody response by a displayed form on an M13 phage in mice. *J. Neuroimmunol.* **236,** 27–38
15. Hashiguchi, S., Nakashima, T., Nitani, A., Yoshihara, T., Yoshinaga, K., Ito, Y., Maeda, Y., and Sugimura, K. (2003) Human FcεRIα-specific human single-chain Fv (scFv) antibody with antagonistic activity toward IgE/FcεRIα-binding. *J. Biochem.* **133,** 43–49
16. Yoshihara, T., Takiguchi, S., Kyuno, A., Tanaka, K., Kuba, S., Hashiguchi, S., Ito, Y., Hashimoto, T., Iwatsubo, T., Tsuyama, S., Nakashima, T., and Sugimura, K. (2008) Immunoreactivity of phage library-derived human single-chain antibodies to amyloid β conformers *in vitro*. *J. Biochem.* **143,** 475–486
17. Williamson, R. A., Peretz, D., Smorodinsky, N., Bastidas, R., Serban, H., Mehlhorn, I., DeArmond, S. J., Prusiner, S. B., and Burton, D. R. (1996) Circumventing tolerance to generate autologous monoclonal antibodies to the prion protein. *Proc. Natl. Acad. Sci. U.S.A.* **93,** 7279–7282
18. Williamson, R. A., Peretz, D., Pinilla, C., Ball, H., Bastidas, R. B., Rozenshteyn, R., Houghten, R. A., Prusiner, S. B., and Burton, D. R. (1998) Mapping the prion protein using recombinant antibodies. *J. Virol.* **72,** 9413–9418
19. Peretz, D., Williamson, R. A., Matsunaga, Y., Serban, H., Pinilla, C., Bastidas, R. B., Rozenshteyn, R., James, T. L., Houghten, R. A., Cohen, F. E.,

Prusiner, S. B., and Burton, D. R. (1997) A conformational transition at the N terminus of the prion protein features in formation of the scrapie isoform. *J. Mol. Biol.* **273,** 614–622
20. Gerber, R., Tahiri-Alaoui, A., Hore, P. J., and James, W. (2007) Oligomerization of the human prion protein proceeds via a molten globule intermediate. *J. Biol. Chem.* **282,** 6300–6307
21. Boel, E., Verlaan, S., Poppelier, M. J., Westerdaal, N. A., Van Strijp, J. A., and Logtenberg, T. (2000) Functional human monoclonal antibodies of all isotypes constructed from phage display library-derived single-chain Fv antibody fragments. *J. Immunol. Methods* **239,** 153–166
22. Yoshinaga, K., Matsumoto, M., Torikai, M., Sugyo, K., Kuroki, S., Nogami, K., Matsumoto, R., Hashiguchi, S., Ito, Y., Nakashima, T., and Sugimura, K. (2008) Ig L-chain shuffling for affinity maturation of phage library-derived human anti-human MCP-1 antibody blocking its chemotactic activity. *J. Biochem.* **143,** 593–601
23. Liu, C., Dalby, B., Chen, W., Kilzer, J. M., and Chiou, H. C. (2008) Transient transfection factors for high-level recombinant protein production in suspension cultured mammalian cells. *Mol. Biotechnol.* **39,** 141–153
24. Zahn, R., Liu, A., Lührs, T., Riek, R., von Schroetter, C., López García, F., Billeter, M., Calzolai, L., Wider, G., and Wüthrich, K. (2000) NMR solution structure of the human prion protein. *Proc. Natl. Acad. Sci. U.S.A.* **97,** 145–150
25. Ishikawa, K., Doh-ura, K., Kudo, Y., Nishida, N., Murakami-Kubo, I., Ando, Y., Sawada, T., and Iwaki, T. (2004) Amyloid imaging probes are useful for detection of prion plaques and treatment of transmissible spongiform encephalopathies. *J. Gen. Virol.* **85,** 1785–1790
26. Atarashi, R., Sim, V. L., Nishida, N., Caughey, B., and Katamine, S. (2006) Prion strain-dependent differences in conversion of mutant prion proteins in cell culture. *J. Virol.* **80,** 7854–7862
27. Féraudet, C., Morel, N., Simon, S., Volland, H., Frobert, Y., Créminon, C., Vilette, D., Lehmann, S., and Grassi, J. (2005) Screening of 145 anti-PrP monoclonal antibodies for their capacity to inhibit PrPSc replication in infected cells. *J. Biol. Chem.* **280,** 11247–11258
28. Kristiansen, M., Messenger, M. J., Klöhn, P. C., Brandner, S., Wadsworth, J. D., Collinge, J., and Tabrizi, S. J. (2005) Disease-related prion protein forms aggresomes in neuronal cells leading to caspase activation and apoptosis. *J. Biol. Chem.* **280,** 38851–38861
29. Veith, N. M., Plattner, H., Stuermer, C. A., Schulz-Schaeffer, W. J., and Bürkle, A. (2009) Immunolocalisation of PrP^{Sc} in scrapie-infected N2a mouse neuroblastoma cells by light and electron microscopy. *Eur. J. Cell Biol.* **88,** 45–63
30. Goold, R., Rabbanian, S., Sutton, L., Andre, R., Arora, P., Moonga, J., Clarke, A. R., Schiavo, G., Jat, P., Collinge, J., and Tabrizi, S. J. (2011) Rapid cell-surface prion protein conversion revealed using a novel cell system. *Nat. Commun.* **2,** 281
31. Sasaki, K., Gaikwad, J., Hashiguchi, S., Kubota, T., Sugimura, K., Kremer, W., Kalbitzer, H. R., and Akasaka, K. (2008) Reversible monomer-oligomer transition in human prion protein. *Prion* **2,** 118–122
32. Pankiewicz, J., Prelli, F., Sy, M. S., Kascsak, R. J., Kascsak, R. B., Spinner, D. S., Carp, R. I., Meeker, H. C., Sadowski, M., and Wisniewski, T. (2006) Clearance and prevention of prion infection in cell culture by anti-PrP antibodies. *Eur. J. Neurosci.* **23,** 2635–2647
33. Korth, C., Stierli, B., Streit, P., Moser, M., Schaller, O., Fischer, R., Schulz-Schaeffer, W., Kretzschmar, H., Raeber, A., Braun, U., Ehrensperger, F., Hornemann, S., Glockshuber, R., Riek, R., Billeter, M., Wüthrich, K., and Oesch, B. (1997) Prion (PrPSc)-specific epitope defined by a monoclonal antibody. *Nature* **390,** 74–77
34. Ushiki-Kaku, Y., Endo, R., Iwamaru, Y., Shimizu, Y., Imamura, M., Masujin, K., Yamamoto, T., Hattori, S., Itohara, S., Irie, S., and Yokoyama, T. (2010) Tracing conformational transition of abnormal prion proteins during interspecies transmission by using novel antibodies. *J. Biol. Chem.* **285,** 11931–11936
35. Beringue, V., Vilette, D., Mallinson, G., Archer, F., Kaisar, M., Tayebi, M., Jackson, G. S., Clarke, A. R., Laude, H., Collinge, J., and Hawke, S. (2004) PrPSc binding antibodies are potent inhibitors of prion replication in cell lines. *J. Biol. Chem.* **279,** 39671–39676
36. Stanker, L. H., Serban, A. V., Cleveland, E., Hnasko, R., Lemus, A., Safar, J., DeArmond, S. J., and Prusiner, S. B. (2010) Conformation-dependent high-affinity monoclonal antibodies to prion proteins. *J. Immunol.* **185,** 729–737
37. Skrlj, N., Vranac, T., Popović, M., Curin Šerbec, V., and Dolinar, M. (2011) Specific binding of the pathogenic prion isoform: development and characterization of a humanized single-chain variable antibody fragment. *PLoS One* **6,** e15783
38. Kosmač, M., Koren, S., Giachin, G., Stoilova, T., Gennaro, R., Legname, G., and Serbec, V. Č. (2011) Epitope mapping of a PrP(Sc)-specific monoclonal antibody: identification of a novel C-terminally truncated prion fragment. *Mol. Immunol.* **48,** 746–750
39. Sasamori, E., Suzuki, S., Kato, M., Tagawa, Y., and Hanyu, Y. (2010) Characterization of discontinuous epitope of prion protein recognized by the monoclonal antibody T2. *Arch. Biochem. Biophys.* **501,** 232–238
40. Horiuchi, M., Karino, A., Furuoka, H., Ishiguro, N., Kimura, K., and Shinagawa, M. (2009) Generation of monoclonal antibody that distinguishes PrP^{Sc} from PrP^{C} and neutralizes prion infectivity. *Virology* **394,** 200–207
41. Saá, P., Castilla, J., and Soto, C. (2006) Ultra-efficient replication of infectious prions by automated protein misfolding cyclic amplification. *J. Biol. Chem.* **281,** 35245–35252
42. Sandberg, M. K., Al-Doujaily, H., Sharps, B., Clarke, A. R., and Collinge, J. (2011) Prion propagation and toxicity *in vivo* occur in two distinct mechanistic phases. *Nature* **470,** 540–542
43. Hnasko, R., Serban, A. V., Carlson, G., Prusiner, S. B., and Stanker, L. H. (2010) Generation of antisera to purified prions in lipid rafts. *Prion* **4,** 94–104
44. D'Castro, L., Wenborn, A., Gros, N., Joiner, S., Cronier, S., Collinge, J., and Wadsworth, J. D. (2010) Isolation of proteinase K-sensitive prions using pronase E and phosphotungstic acid. *PLoS One* **5,** e15679
45. Anaya, Z. E., Savistchenko, J., Massonneau, V., Lacroux, C., Andréoletti, O., and Vilette, D. (2011) Recovery of small infectious PrP(res) aggregates from prion-infected cultured cells. *J. Biol. Chem.* **286,** 8141–8148
46. Cronier, S., Gros, N., Tattum, M. H., Jackson, G. S., Clarke, A. R., Collinge, J., and Wadsworth, J. D. (2008) Detection and characterization of proteinase K-sensitive disease-related prion protein with thermolysin. *Biochem. J.* **416,** 297–305
47. Biasini, E., Seegulam, M. E., Patti, B. N., Solforosi, L., Medrano, A. Z., Christensen, H. M., Senatore, A., Chiesa, R., Williamson, R. A., and Harris, D. A. (2008) Non-infectious aggregates of the prion protein react with several PrP^{Sc}-directed antibodies. *J. Neurochem.* **105,** 2190–2204
48. Saborio, G. P., Permanne, B., and Soto, C. (2001) Sensitive detection of pathological prion protein by cyclic amplification of protein misfolding. *Nature* **411,** 810–813
49. Uryu, M., Karino, A., Kamihara, Y., and Horiuchi, M. (2007) Characterization of prion susceptibility in Neuro2a mouse neuroblastoma cell subclones. *Microbiol. Immunol.* **51,** 661–669
50. Prusiner, S. B., Groth, D. F., Bolton, D. C., Kent, S. B., and Hood, L. E. (1984) Purification and structural studies of a major scrapie prion protein. *Cell* **38,** 127–134

SUPPLEMENTAL DATA

Figure S1. Scheme for construction of expression vector of heavy chain of PRB7 scFv fragments.
The details were described in Experimental procedures.

Figure S2. Scheme for construction of expression vector of light chain of PRB7 scFv fragments.
The details were described in Experimental procedures.

Figure S3. Molecular model
A. Molecular model of PRB7 scFv. PRB7 scFv was simulated with 2GHWD (anti SARS spike protein receptor antibody, PDB) as template. B. Fab domain molecular modeling of PRB7 IgG was simulated by use of Molecular Operating EnvironmentTM (MOE, Version 2009.10). Each template and PDB code was showed by Homology analysis of MOE. Template of PRB7 H-chain variable domain: flanking region; 1HEZ.B, CDR1; 1NLO.H, CDR2; 2GHW.DH, CDR3; 4FAB.H Template of PRB7 light-chain variable domain: flanking region; 1HEZ.A, CDR1; 1ZLS.L, CDR2; 1U6A.L, CDR3; 1DNO.C. The complementary determining regions (CDR1-CDR3) and the flanking regions (FR1-4) were deduced according to IMGT [http://www.imgt.cines.fr/]; VH domain (white), VH-CDR1 (red), VH-CDR2 (blue), VH-CDR3 (orange), VL domain (gray), VL-CDR1 (magenda), VL-CDR2 (skyblue), VL-CDR3 (yellow).

Figure S4. The binding specificity of PRB7 or PRB30 was not changed by pH of incubation buffer of ELISA.
β-form PrP of α-PrP (100 ng/40 μl) was coated on ELISA plates using refolding buffers of either pH4 or pH8. After washing plates, PRB7 or PRB30 was added and incubated in wells using either pH4 incubation buffer or pH8 incubation buffer (10 mM Tris-acetate buffer with 10 mM Na acetate buffer) at room temperature. The binding of PRB7 or PRB30 was detected as described in Experimental procedures.

Figure S5. PRB7 IgGreacts with β-form PrP separated by native gel under non-reducing codition.
We performed Immunogel-ELISA which was developed by us to determine whether PRB7 IgG reacts with non-denatured β-form PrP (1). A. PrP conformers were not resolved by native PAGE under usual pH condition (pH8.8) as they stucked to top wells without running. Therefore, native page was performed at pH 4.8 (unpublished data). Briefly, α-form or β-form of human PrPs (2 μg/lane) were loaded to 6.5% polyacrylamid gel. In this panel, gel staining was carried out with Coomassie Brilliant Blue (CBB: Nacalai Tesque, Kyoto, Japan). B. The scheme of immunogel-ELISA is presented (1). Briefly, gel slices containing PrP conformers were excised. Each gel fraction was placed in 1.5 ml-tubes (Quality Scientific Plastics, CA, USA) punched with a 27G needle (TERUMO, Tokyo, Japan) and crushed by pushing them through the pore using the gasket of a 1 ml-syringe (TERUMO, Tokyo, Japan). Each gel fragment was incubated with PBS in ELISA plate overnight at 4 °C. The gel fragments were discarded from ELISA plates, and the immunoplates were blocked with PBS containing 0.25% BSA for 1 h at room temperature. The PRB7 scFv (2 μg/ml) was added to each well and plates were incubated for 1 h at room temperature. PRB7 scFv was detected with anti-E tag Antibody (1:1000) in combination with a AP-conjugated goat anti mouse IgG Antibodies (1:2000). Absorbance was measured at 405 nm in incubation with 50 μl of a p-nitrophenyl phosphate/10% diethanol amine solution by use of a microplate reader (NJ-2300; Tokyo, Japan). C. According to the scheme of panel B, PrP conformers recovered from non-reduced, native PAGE were coated in ELISA plates. These PrPs were detected by PRB7 scFv or SAF32. As shown in panel A, fraction α1 was resolved from α-form PrP. Fraction β1 or β2 was resolved from β-form PrP. "gel" indicates samples derived from native gel alone. Although the amount of protein per well was variable in α1, β1 or β2 fractions, the identical sample was tested in replicated experiments by using

either PRB7 scFv or SAF32.

Figure S6. Living or fixed cells were not directly stained with PRB7 IgG.
In the case of living cells, ScN2a cells were blocked with 3% BSA/0.1 % azide/PBS for 30 min at room temperature. Blocked cells were incubated with PRB7 IgG (green), control human IgG/κ (green) or SAF32 (red, 5 μg/ml). In the case of fixed cells, ScN2a cells were fixed with paraformaldehyde, permeated and blocked. Fixed cells were incubated with PRB7 IgG (green), control human IgG/κ (green) or SAF32 (red, 5 μg/ml). Cells were stained with AlexaFluor 488-labeled anti-human IgG, AlexaFluor 546-labeled anti-mouse IgG, or DAPI (blue).

Figure S7. β-form PrP can be sandwiched with PRB7 IgG and SAF32 or 6D11 in ELISA.
A, B. Antibody (PRB7 IgG or control human IgG/κ: 100 ng/50 μl) were incubated with human β-form PrP (100 ng/40 μl) in a pH 4.0-folding buffer for 1 h and then added into wells precoated with an anti-PrP mAb, SAF32 or 6D11 (100 ng/50 ml). After treatment with a blocking and washing solution, the bound antibody was detected using an HRP-conjugated anti-human IgG.

BIBLIOGRAPHY

1. Hamasaki, T., Uchida, S., Yoshihara, T., Hashiguchi, S., Ito, Y., and Sugimura, K. (2007) *Biol Pharm Bull* **30**, 1361-1364

Figure S1

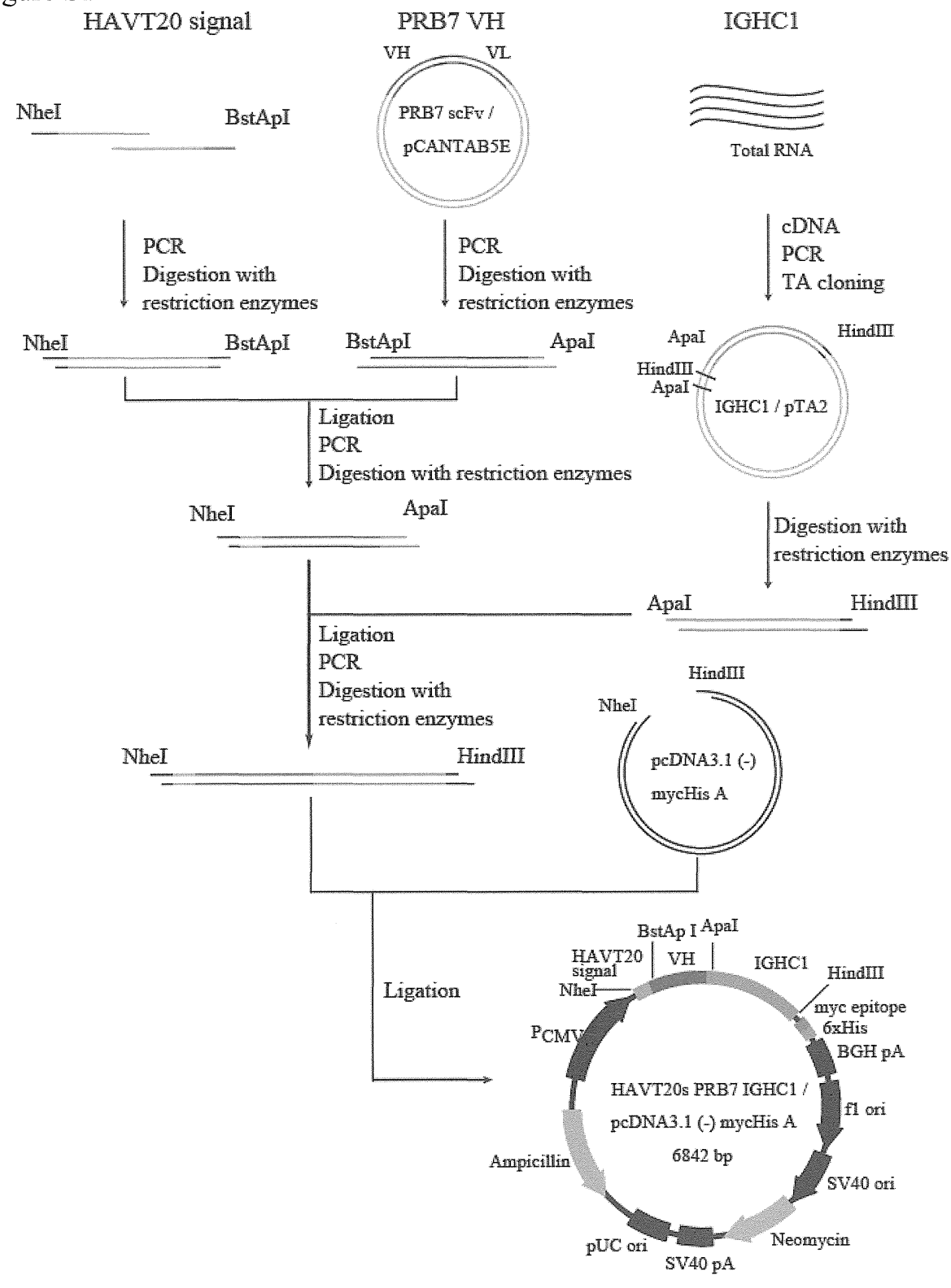

Figure S2

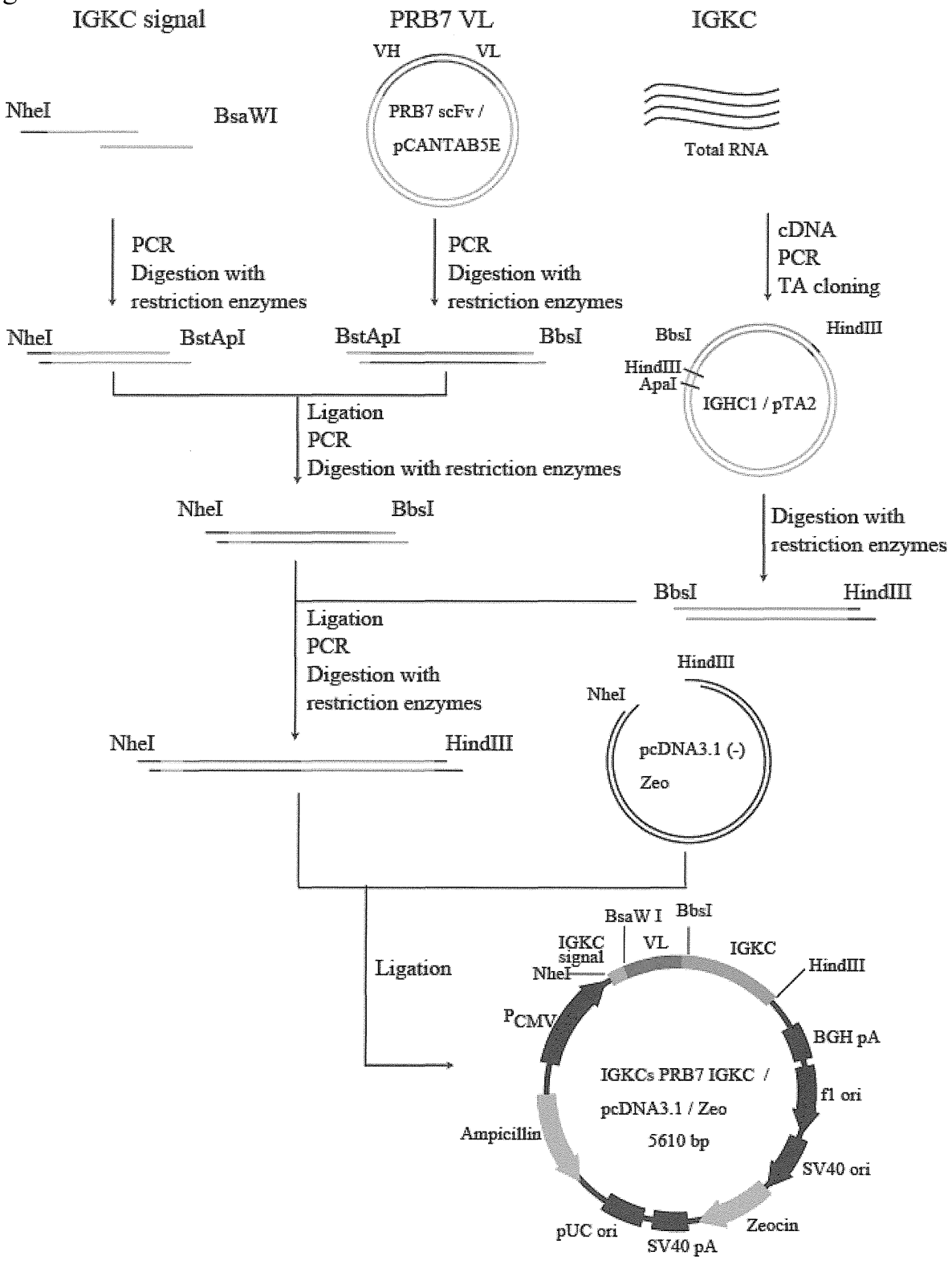

Figure S3

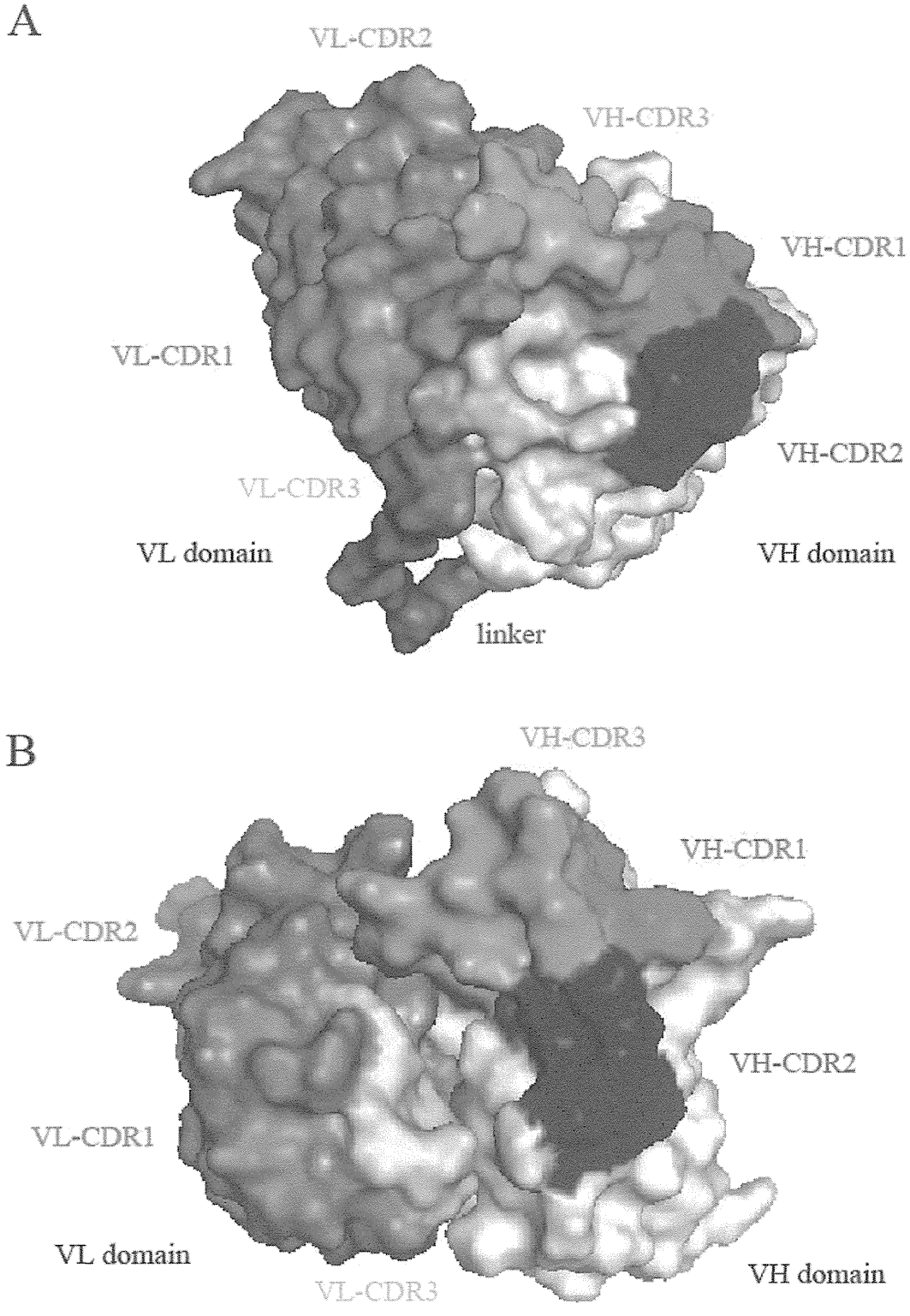

Figure S4

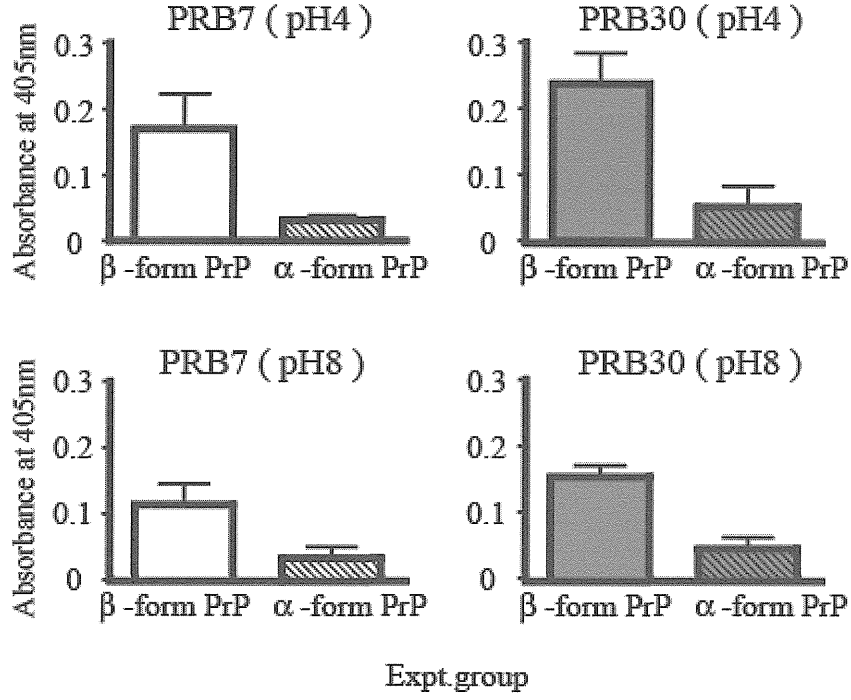

Figure S5

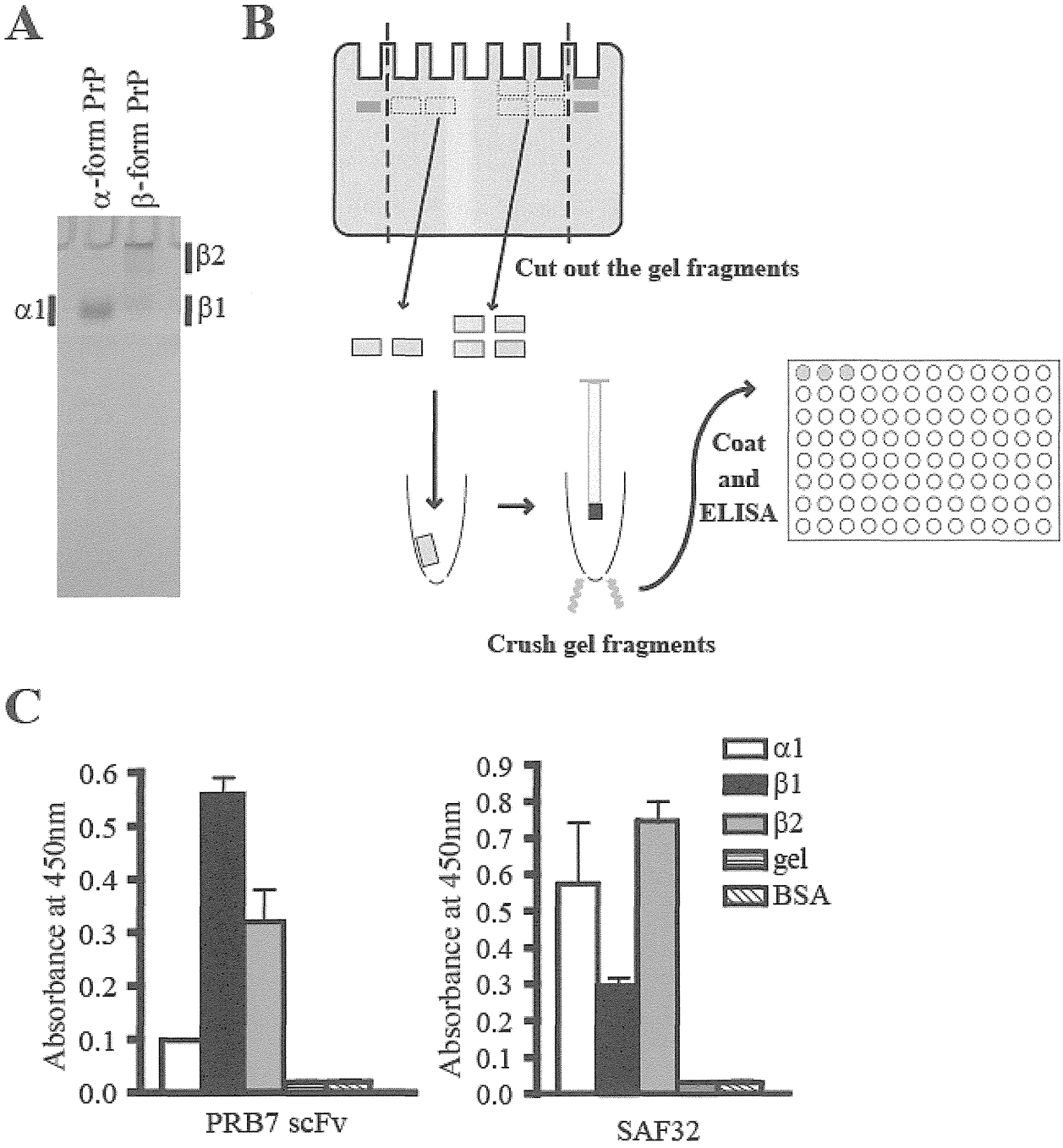

Figure S6

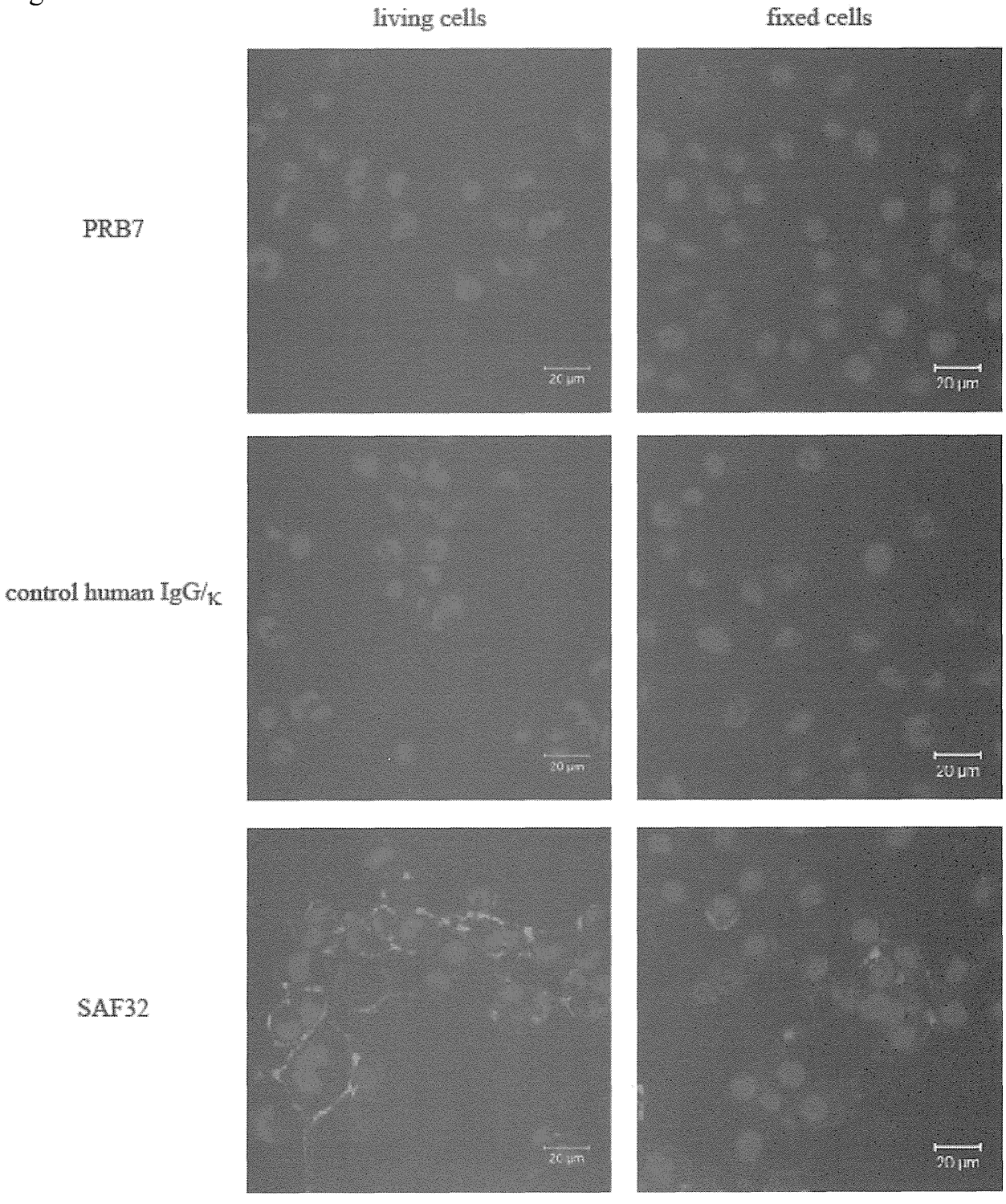

Figure S7

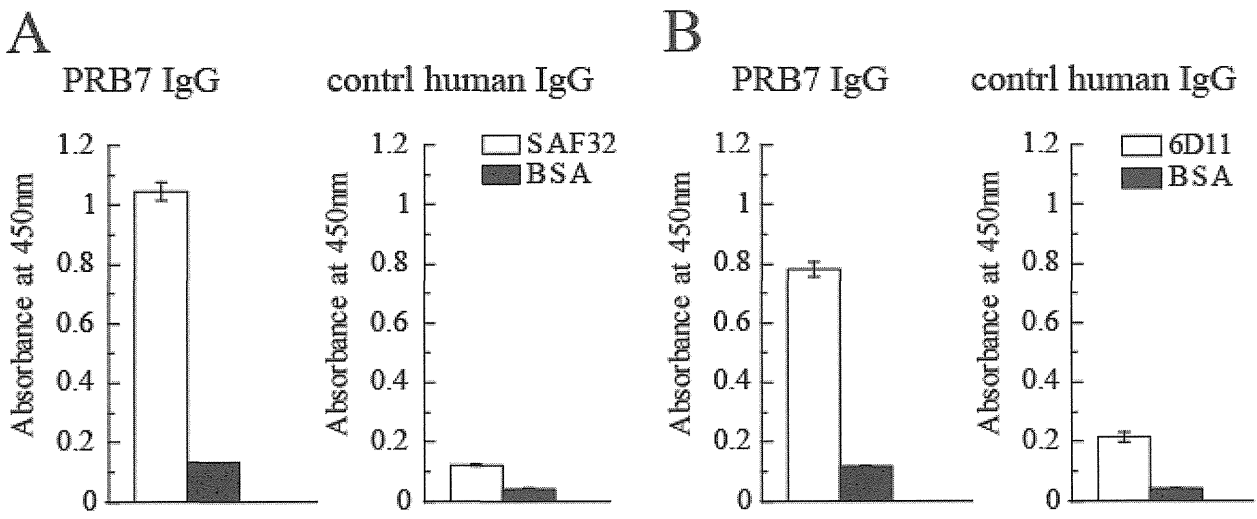

NEUROPATHOLOGY

Neuropathology 2012; **32**, 124–132 doi:10.1111/j.1440-1789.2011.01245.x

Original Article

Protease-resistant PrP and PrP oligomers in the brain in human prion diseases after intraventricular pentosan polysulfate infusion

Hiroyuki Honda,[1] Kensuke Sasaki,[1] Haruhiko Minaki,[1] Kenta Masui,[1] Satoshi O. Suzuki,[1] Katsumi Doh-ura[2] and Toru Iwaki[1]

[1]Department of Neuropathology, Graduate School of Medical Sciences, Kyushu University, Fukuoka and [2]Department of Neurochemistry, Tohoku University Graduate School of Medicine, Sendai, Japan.

Intraventricular infusion of pentosan polysulfate (PPS) as a treatment for various human prion diseases has been applied in Japan. To evaluate the influence of PPS treatment we performed pathological examination and biochemical analyses of PrP molecules in autopsied brains treated with PPS (one case of sporadic Creutzfeldt-Jakob disease (sCJD, case 1), two cases of dura mater graft-associated CJD (dCJD, cases 2 and 4), and one case of Gerstmann-Sträussler-Scheinker disease (GSS, case 3). Six cases of sCJD without PPS treatment were examined for comparison. Protease-resistant PrP (PrP^{res}) in the frontal lobe was evaluated by Western blotting after proteinase K digestion. Further, the degree of polymerization of PrP molecules was examined by the size-exclusion gel chromatography assay. PPS infusions were started 3–10 months after disease onset, but the treatment did not achieve any clinical improvements. Postmortem examinations of the treated cases revealed symmetrical brain lesions, including neuronal loss, spongiform change and gliosis. Noteworthy was GFAP in the cortical astrocytes reduced in all treated cases despite astrogliosis. Immunohistochemistry for PrP revealed abnormal synaptic deposits in all treated cases and further plaque-type PrP deposition in case 3 of GSS and case 4 of dCJD. Western blotting showed relatively low ratios of PrP^{res} in case 2 of dCJD and case 3 of GSS, while in the treated sCJD (case 1), the ratio of PrP^{res} was comparable with untreated cases. The indices of oligomeric PrP were reduced in one sCJD (case 1) and one dCJD (case 2). Although intraventricular PPS infusion might modify the accumulation of PrP oligomers in the brains of patients with prion diseases, the therapeutic effects are still uncertain.

Key words: Creutzfeldt-Jakob disease, oligomer, pentosan polysulfate, prion protein, size-exclusion gel chromatography.

INTRODUCTION

Prion diseases, also known as transmissible spongiform encephalopathies (TSEs), are fatal neurodegenerative disorders that include Creutzfeldt-Jakob disease (CJD) and Gerstmann-Sträussler-Scheinker disease (GSS) in humans, and scrapie and bovine spongiform encephalopathy in animals. In these diseases, histopathological changes in the brain are characterized by spongiform change, reactive changes of astrocytes and variable loss of neurons.[1] In addition, deposition of a protease-resistant isoform of prion protein (PrP^{res}) is detected in the brain. This PrP^{res} contains high β-sheet content and is composed of polymerized PrP molecules post-translationally converted from normal, cellular PrP (PrP^{c}) of 254-amino acid 32–35 kDa glycolipid-anchored, plasma membrane protein that is widely expressed in the CNS.[2]

There is currently no effective remedy for human prion diseases, but several therapeutic compounds including quinacrine and pentosan polysulfate (PPS) have been tested for patients with prion diseases on experimental trial bases. Quinacrine is reportedly effective in inhibiting PrP^{res} formation in prion-infected cells.[3,4] However, subsequent studies showed no apparent beneficial effects of quinacrine in either experimental animals or humans.[5–7] By comparison, PPS has been shown to prevent the propagation of

Correspondence: Hiroyuki Honda, MD, Department of Neuropathology, Graduate School of Medical Sciences, Kyushu University, 3-1-1 Maidashi, Higashi-ku, Fukuoka 812-8582, Japan. Email: h-hiroyu@np.med.kyushu-u.ac.jp

Received 28 May 2011; revised 23 June 2011 and; accepted 25 June 2011; published online 1 August 2011.

PrP^{res} in prion-infected cells.[8] Additionally, in experimental animals PPS has been administered directly into the CNS via an intra-hemiventricular canula, resulting in significant prolongation of the incubation periods accompanied with the laterality of neuropathological changes.[9] PPS inhibits PrP^{res} formation by interfering with the interaction of PrP^{c} and PrP^{res} with endogenous glycosaminoglycan or proteoglycan.[10] In addition, PPS stimulates endocytosis of PrP^{c}, reducing the amount of PrP^{c} present on the cell surface.[11] Experimental trials of intraventricular PPS infusion in the patients with prion diseases have been performed on observational bases, and thus it has been difficult to prove its efficacy.[12,13] In fact, Tsuboi *et al.* reported that PPS treatment showed no apparent improvements of clinical features in Japanese patients with prion disease.[14] In comparison, Bone *et al.* reported that mean survival of seven patients with PPS treatment was longer than reported values for the natural history of prion diseases in the United Kingdom, although possible reasons for this finding remain unclear.[15]

The main pathogenic component in prion diseases has been suggested to be PrP^{res} composed of PrP polymers. Recently, PrP oligomers, equivalent to 14–28 PrP molecules were reported as the most infectious units.[16,17] In addition, Kristiansen *et al.* reported that disease-associated PrP oligomers inhibit the 26S proteasome and cause neurotoxicity.[18] We have previously developed a gel-filtration chromatography method using spin columns to examine PrP oligomers, and revealed that increased PrP oligomers correlated with the degree of histopathological changes such as spongiform change and gliosis.[19] In other neurodegenerative diseases, including Alzheimer's disease, dementia with Lewy bodies and Parkinson's disease, soluble oligomers of amyloidogenic proteins were proposed to be the principal neurotoxic agents.[20,21]

In this report, to clarify the influence of PPS treatment on brains affected with piron diseases, we performed pathological examination and biochemical analyses of PrP, including its degree of polymerization, in four cases of prion diseases treated with PPS.

MATERIALS AND METHODS

We investigated the degree of polymerization of PrP molecules in four prion diseases cases that received PPS treatment, denoted PPS(+): one case of sporadic CJD (sCJD), two cases of dura mater graft-associated CJD (dCJD), and one case of GSS. We also examined six cases of sCJD without PPS treatment, denoted PPS(–), for comparison. The profiles of the patients are summarized in Table 1. At autopsy the brains were weighed and fixed with 10% buffered formalin. Six micrometer-thick sections of paraffin-embedded tissue from the CNS were stained with HE and the KB staining method. Immunohistochemistry was performed with primary antibodies against anti-prion antibody (mouse monoclonal 3F4, 1:400; Signet, Dedham, MA, USA) and GFAP (rabbit polyclonal, 1:1000; Dako, Glostrup, Denmark). The sections were then treated with appropriate biotinylated secondary antibodies and the reaction products were detected using the avidin-biotinylated peroxidase complex method (ABC; Vector Laboratories, Burlingame, CA, USA) coupled with a diaminobenzidine (Dojindo, Kumamoto, Japan) reaction.

Brain homogenate preparation

Human brains were collected at autopsy from four prion disease cases that had received PPS treatment and six cases of sCJD that had not received PPS treatment. Samples of frontal cortex were frozen fresh and stored at –80°C until used. The brain samples were homogenized to a final concentration of 10% in lysis buffer with sodium dodecyl sulfate (SDS) (100 mM Tris-HCl, 100 mM NaCl, 10 mM EDTA, 1% SDS, pH 7.6) for the size-exclusion gel chromatography assay. Most PrP^{c} could be solubilized as monomers in lysis buffer with SDS.[19] Samples were homogenized

Table 1 Summary of patient profiles

Case	Diagnosis	Genotype/PrP^{res} type	Age at death	Sex	Duration of illness (months)	Duration of PPS treatment (months)	Brain weight (g)
1	sCJD	129MM/type 1	74	F	23	20	660
2	dCJD	129MM/type 1	67	M	12	9	950
3	GSS	P102L/8 kDa	70	F	20	14	1055
4	dCJD	129MM/type 1	55	M	14	4	1460
5	sCJD	129MM/type 1	71	M	10	–	562
6	sCJD	129MM/type 1	61	M	30	–	745
7	sCJD	129MM/type 1	69	M	15	–	940
8	sCJD	129MM/type 1	73	F	4	–	1100
9	sCJD	129MM/type 1	68	F	2	–	1260
10	sCJD	NA/type 1	66	M	2.5	–	1435

dCJD, dura CJD; F, female; GSS, Gerstmann-Sträussler-Scheinker disease; M, male; MM, methionine homozygote at prion protein gene codon 129; NA, not available; PPS, pentosan polysulfate; PrP^{res}, proteinase resistant isoform of prion protein; sCJD, sporadic CJD.

at 5000 rpm for 30 s in a bead disrupter homogenizing system (MicroSmash MS-100; Tomy Seiko Co., Ltd, Tokyo, Japan). Homogenates were then clarified by centrifugation at 250 *g* for 5 min and the supernatant was stored at –80°C.

Detection of PrP^{res}

Conventional procedure for the detection of PrP^{res} was conducted as follows: 1% brain homogenate was prepared in extraction buffer (100 mM Tris-HCl, 100 mmol NaCl, 10 mmol EDTA, 0.5% Nonidet P-40, 0.5% sodium deoxycholate, pH 7.6) and incubated with 50 μg/mL proteinase K (PK) at 37°C for 1 h. Protease activity was then abolished by the addition of 1 mmol Pefabloc SC (Roche, Indianapolis, IN, USA). Undigested PrP^{res} fragments were separated by SDS-PAGE in 12% NuPAGE Bis-Tris gels (Invitrogen, Carlsbad, CA, USA) and transferred onto polyvinylidene difluoride membranes (Immobilon-P; Millipore, Billerica, MA, USA). PrP was detected using anti-PrP antibody (mouse monoclonal 3F4, 1:10 000) as the primary antibody and peroxidase-conjugated anti-mouse IgG as the secondary antibody (AP192P, 1:20 000; Chemicon, Temecula, CA, USA). The immunoreaction was visualized using the ECL plus Western Blotting Detection System (GE Healthcare; Chalfont St. Giles, Buckinghamshire, UK).

Size-exclusion gel chromatography assay

We performed the size-exclusion gel chromatography assay using the spin-column kit CHROMA SPIN-200 (Clontech, San Francisco, CA, USA) that clearly separated oligomeric PrP from monomeric PrP.[19,22] The samples were first centrifuged at 120 *g* for 2 min, and the first fraction was collected in the collection tube. Another 40 μL of lysis buffer was added, and the samples were centrifuged at 120 *g* for 2 min to collect the size-exclusion fractions sequentially. In these operations, we used a centrifuge with a swing-bucket rotor (A-4–62; Eppendorf, Hamburg, Germany). Fractionated PrP was detected without PK treatment by SDS-PAGE and Western blot analysis, as described above.

RESULTS

Case reports and brain pathology

Details of PPS treatment and clinical findings from the patients were described in a previous paper.[14] In all four PPS-treated cases, the PPS infusion catheter was inserted into the right lateral ventricle, and the PPS dose was gradually escalated to the target dosage of 120 μg/kg/day. PPS treatment showed no apparent improvement of clinical features in all the cases. Clinicopathological findings from each case that had received PPS treatment are described below.

Case 1

A 72-year-old woman showed truncal ataxia and progressive gait disturbance. She had no family history of prion or neurological disease. Diffusion weighted imaging (DWI) demonstrated diffuse bilateral high-intensity signals in the cerebral cortex and striatum. Periodic synchronous discharge was seen in electroencephalography 2 months after disease onset. She was diagnosed with sCJD. Myoclonus and startle reaction were observed 3 months after the onset. The PPS infusion was started 3 months after the onset; however, no improvement in clinical features was observed. She developed akinetic mutism 6 months after the onset. Tonic seizures in extremities were also seen. The patient died of pneumonia and autopsy was performed 14.5 h after death. The brain weighed 660 g and showed severe atrophy with bilateral subdural hematoma and fluid collection. Microscopy demonstrated severe neuronal loss, rarefaction of neuropil, and gliosis across the cerebral cortices (Fig. 1A). Although astrocytosis was noted in HE staining, GFAP expression was weak in the cerebral cortices, except in subpial astrocytes (Fig. 2A). These pathological changes were also seen in the basal ganglia and thalamus. Synaptic PrP deposition was detected in the cerebral cortices, basal ganglia and thalamus (Fig. 1B). There was no laterality of spongiform change, neuronal loss, gliosis or PrP deposition.

Case 2

A 66-year-old man showed dysarthria 25 years after dura mater graft implantation because of cerebral hemorrhage. He manifested right hand clumsiness and progressive gait disturbance. Myoclonus was also seen in the right extremities. He had no family history of prion disease or neurological disease. DWI showed abnormal high-intensity signals in bilateral temporal cortices. In addition, brain biopsy was performed and revealed a type 1 PrP^{res} accumulation. The patient was diagnosed with dCJD. The electroencephalogram showed no periodic synchronous discharges. He developed akinetic mutism 2 months after disease onset. PPS infusion was started 3 months after the onset, but no improvement of clinical features was observed. The patient died of pneumonia and autopsy was performed 9 h after death. The brain weighed 950 g and showed severe atrophy with bilateral subdural fluid collection. Spongiform change, severe neuronal loss and gliosis were seen in the cerebral cortices (Fig. 1C). Astrocytosis was found in all layers of the cerebral cortex; however GFAP expression was weak (Fig. 2B). Synaptic PrP

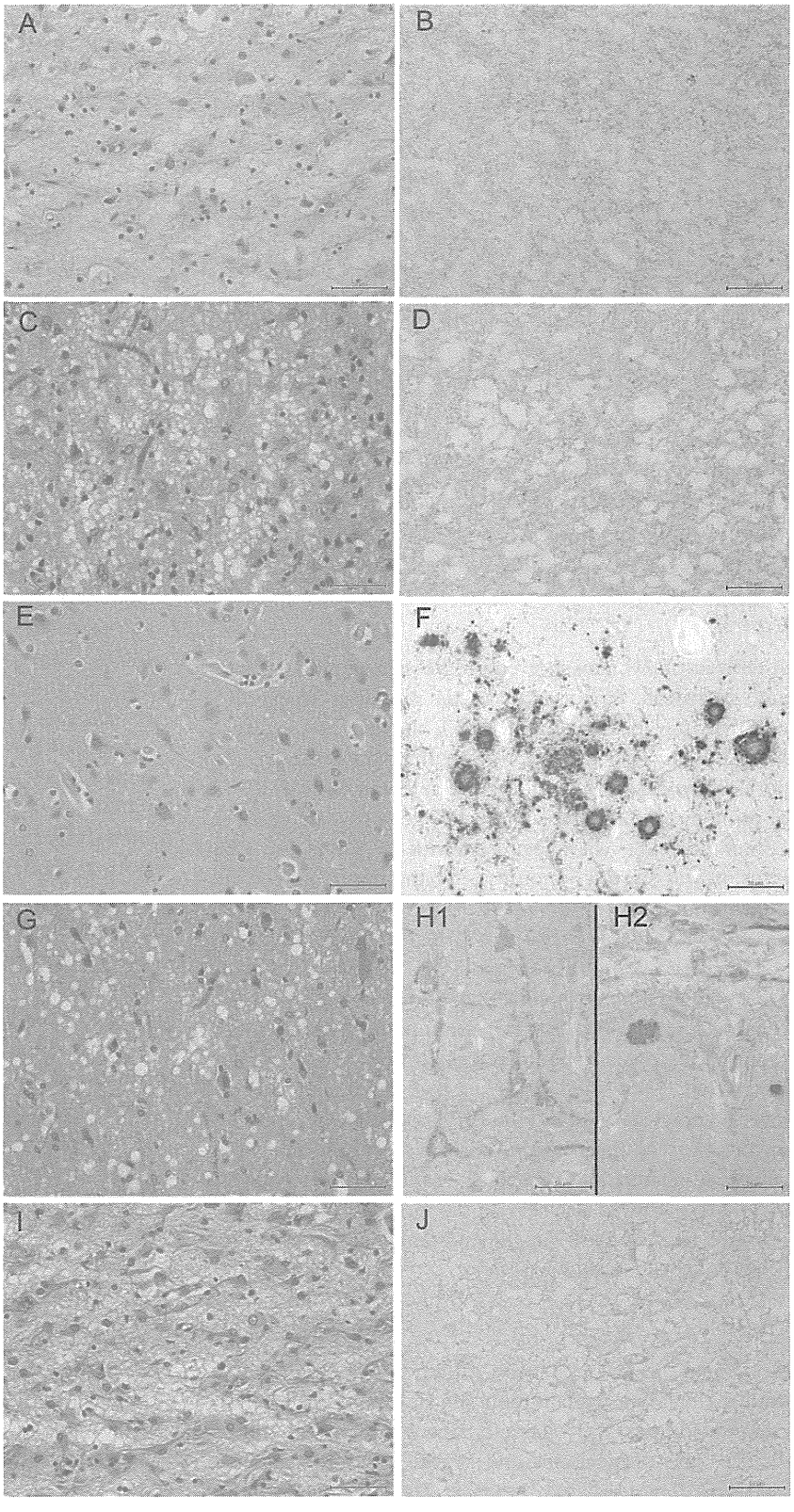

Fig. 1 Light micrographs of frontal cortices in prion diseases. A, C, E, G, I: HE stain. B, D, F, H1, H2, J: immunohistochemistry for PrP. Case 1 shows severe neuronal loss and significant rarefaction of neuropil (A) and synaptic PrP deposition (B). Case 2 shows typical spongiform change (C) and synaptic PrP deposition (D). Case 3 shows several amyloid plaques, neuronal loss and gliosis; however spongiform change is very mild (E). Both plaque-type deposition and synaptic deposition of PrP are detected (F). Case 4 shows neuronal atrophy and spongiform change (G). Synaptic deposition of PrP is mainly seen around pyramidal neurons of the deep cortical layer (H1) and plaque-type depositions are mainly found in the subpial layer (H2). Case 5 without pentosan polysulfate (PPS) treatment shows severe neuronal loss and remarkable rarefaction (I) and synaptic PrP deposition (J).

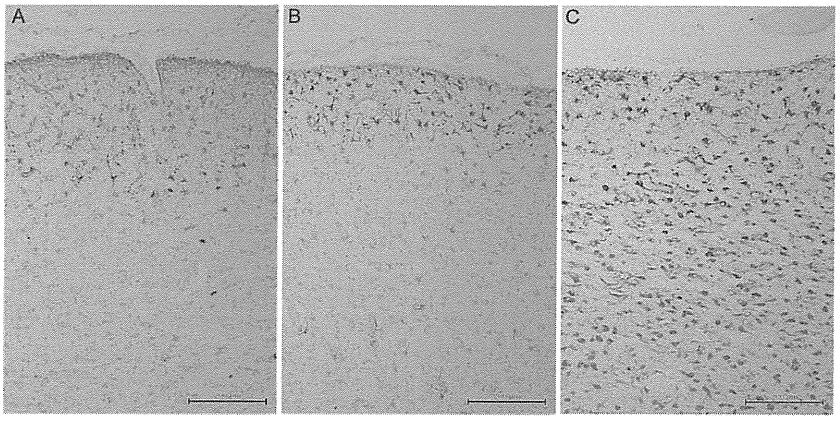

Fig. 2 Immunohistochemistry for GFAP of the frontal cortices. In case 1 (A) and case 2 (B) with pentosan polysulfate (PPS) treatment, subpial astrocytes show strong immunoreactivity for GFAP, but most cortical astrocytes show negative or weak immunoreactivity for GFAP despite their reactive morphology. In comparison, cortical astrocytes in all layers show strong GFAP immunoreactivity in case 5, which did not receive PPS treatment (C).

deposition was also detected in the cerebral cortices (Fig. 1D). No plaque-type deposition of PrP was noted. There was no laterality of spongiform change, neuronal loss, gliosis or PrP deposition.

Case 3

A 68-year-old woman showed progressive gait disturbance and dysarthria. Upper limb ataxia was also observed 5 months after disease onset. DWI showed no apparent intensity changes. The electroencephalogram showed no periodic synchronous discharges. She had a family history of prion disease. Analysis of the PrP gene revealed a P102 L mutation. She was diagnosed with GSS and the PPS infusion was started 6 months after the onset. No clinical improvement was observed. The patient died of pneumonia and autopsy was performed 27 h after death. The brain weighed 1055 g and showed moderate atrophy with bilateral subdural fluid collection. Spongiform change and neuronal loss were mild (Fig. 1E). Although astrocytosis was found in all layers of the cerebral cortices, GFAP immunoreactivity was seen mainly in the superficial cortical layers. Numerous plaque-type PrP depositions were noted in all layers of the cerebral cortices (Fig. 1F), the basal ganglia, thalamus and cerebellar granular layer. Synaptic PrP deposition was also seen in the molecular layer of the cerebral cortices, basal ganglia and thalamus. No laterality of pathological change was seen.

Case 4

A 55-year-old man showed dizziness 19 years after dura mater graft implantation. He developed dysarthria, memory deficits and character changes 8 months after disease onset. Myoclonus and startle reaction were also observed 10 months after the onset. The electroencephalogram showed no periodic synchronous discharges. DWI demonstrated high-intensity signals in the right caudate nucleus and the right thalamus. He had no family history of prion disease or neurological disease. Brain biopsy was performed and showed a type 1 PrP^{res} accumulation. The patient was diagnosed with dCJD. Although PPS infusion was started 10 months after the onset, no clinical improvement was observed. The patient died of pneumonia and autopsy was performed 13 h after death. The brain weighed 1460 g. Right subdural hematoma was noted, but brain atrophy was not apparent. Spongiform change, severe neuronal loss and gliosis were apparent in the precentral gyrus, entorhinal cortex, anterior cingulate gyrus, thalamus and putamen (Fig. 1G). Even in regions where astrocytosis was found in all layers, GFAP immunoreactivity was seen exclusively in the superficial layer of the cerebral cortices. Both synaptic deposition of PrP (Fig. 1H1) and plaque-type deposition of PrP (Figs 1,2) were noted in the cerebral cortices, basal ganglia and hippocampus. There was no laterality of spongiform change, neuronal loss, gliosis or PrP deposition.

In PPS(–) cases, HE staining revealed that the levels of neuronal loss, spongiosis and gliosis advanced in accordance with the loss of brain weight. Various levels of synaptic PrP deposition were noted in each case. In case 5, which showed severe brain atrophy, neuronal loss and rarefaction of neuropils were evident (Fig. 1I). Both astrocytosis and marked GFAP immunoreactivity were noted in all layers of the cerebral cortices (Fig. 2C). Synaptic PrP deposition was also detected in cerebral cortices (Fig. 1J).

The ratio of PrP^{res}/total PrP

Western blot analysis detected PrP^{res} and total PrP. Cases 1 and 2 showed a type 1 pattern (Fig. 3A,B). Case 3 showed PrP^{res} fragments with molecular masses of around 8 kDa (Fig. 3C). Case 4 showed PrP^{res} fragments with intermediate size between types 1 and 2 (Fig. 3D). We calculated the ratio of PrP^{res}/total PrP based on the signal intensities of the immunoblots. In PPS(–) cases, the ratio of PrP^{res}/total PrP was already increased in case 9 with mild brain

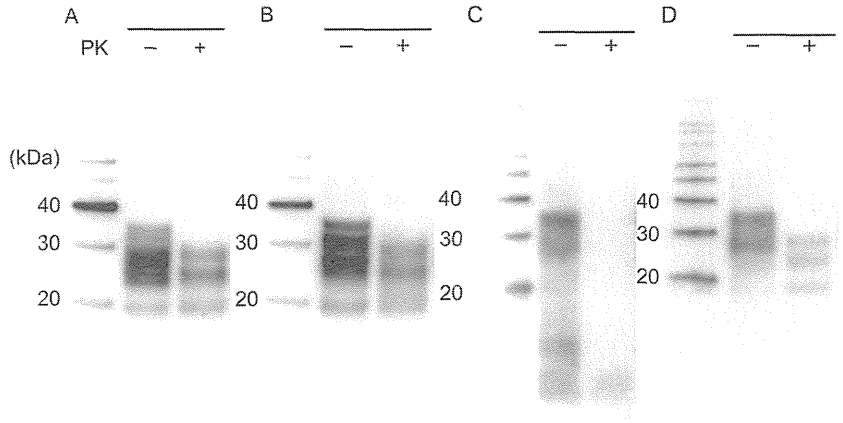

Fig. 3 Western blot analysis for PrP with or without proteinase K (PK) treatment. The brain homogenates from frontal cortices of pentosan polysulfate positive (PPS(+)) cases were separated by SDS-PAGE and probed with anti-PrP antibody (clone 3F4). The blot shows a type 1 pattern of PrP^{res} in case 1 (A) and case 2 (B). Case 3 shows PrP^{res} fragments with molecular masses of around 8 kDa (C). Case 4 shows PrP^{res} fragments with intermediate size between types 1 and 2 (D).

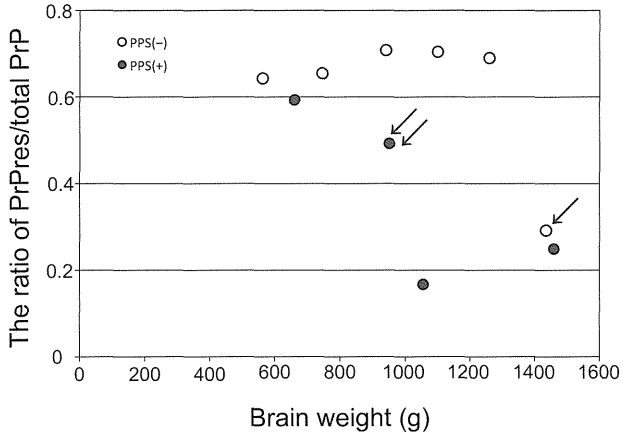

Fig. 4 Relationship between PrP^{res}/total PrP ratio and brain weight. The ratios of PrP^{res}/total PrP are markedly increased in all pentosan polysulfate negative (PPS(–)) cases (open circles) except for case 10 (arrow). Among PPS(+) cases (closed circles), case 2 (double arrows) shows a relatively low ratio of PrP^{res}/total PrP in comparison to PPS(–) cases.

atrophy. Case 2, one of three CJD cases with PPS(+), showed a relatively low ratio of PrP^{res}/total PrP in comparison to PPS(–) cases (Fig. 4).

The indices of oligomeric PrP/total PrP and monomeric PrP/total PrP

The first fraction consisted mostly of the void volume and contained insufficient protein to be assessed. Pre-column samples were taken as loading samples of total PrP. The aggregated forms of PrP were detected in fractions 2–4 (Fig. 5). Fraction 3 in this method represented the oligomeric PrP.[19,22] Thus, the index of oligomeric PrP/total PrP was obtained by dividing the intensity of fraction 3 by the intensity of the pre-column sample. Proteins with molecular weights of approximately 30 kDa, such as monomer PrP molecules, were collected mainly in fractions 6–8.[19,22] Fraction 7 represented the monomeric PrP. The index of monomeric PrP/total PrP was obtained by dividing the intensity of fraction 7 by the intensity of pre-column samples. In PPS(–) cases, the indices of oligomeric PrP/total PrP were increased according to the disease severity (Fig. 6A). Among PPS(+) cases, two CJD cases (cases 1 and 2) showed lower indices of oligomeric PrP/total PrP in comparison to PPS(–) cases. The indices of monomeric PrP/total PrP were decreased markedly in the cases with severe brain weight loss (Fig. 6B). There were no significant differences in the monomer indices between PPS(+) cases and PPS(–) cases.

DISCUSSION

Our post mortem study revealed that the PPS treatment did not apparently improve brain pathology in human prion diseases, although PPS treatment decreased the ratios of PrP^{res}/total PrP and the indices of oligomeric PrP/total PrP in some CJD cases. These findings might be relevant to apparently discrepant clinical findings: one reported no significant clinical improvements in prion diseases with PPS treatment[14,23] and the other reported that longer mean survival time in patients that had received PPS treatment was longer than previously reported for untreated specific prion diseases.[15]

The post mortem examinations revealed that neuronal loss, spongiform change and gliosis were advanced in both PPS(–) and PPS(+) cases with a greater loss of brain weight. In all PPS(+) cases, astrocytosis was evident in all layers of cerebral cortices, but GFAP expression levels were markedly reduced in the cerebral cortices, except in subpial astrocytes. CJD cases without PPS treatment usually showed strong immunoreactivity for GFAP in the cortical astrocytes as observed in case 5. Thus, we treated rat primary astrocytes with several concentrations of PPS (0 μg/mL, 0.4 μg/mL, 2.0 μg/mL, 10 μg/mL), but GFAP

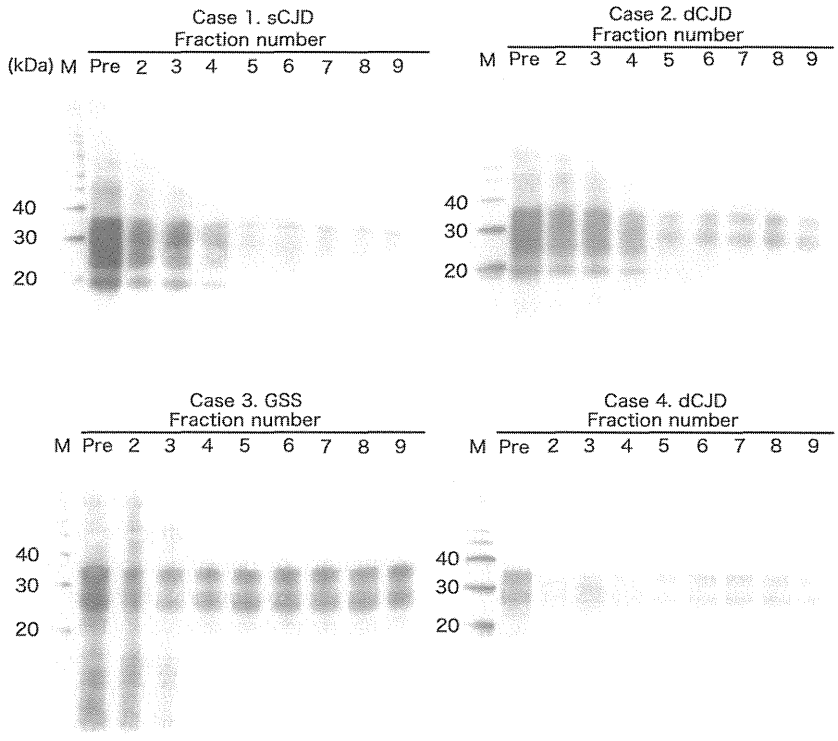

Fig. 5 Fractionation patterns of PrP in prion disease cases treated with PPS. The brain homogenate from the frontal cortex of each case was gel-filtrated without proteinase K (PK) treatment. Oligomeric PrP are detected mainly in fractions 2–4. Monomeric PrP are detected mainly in fractions 6–8. Pre: Pre-column brain homogenate.

expression levels were not significantly altered (data not shown). Therefore, we suggest that decreased GFAP expression levels in cortical astrocytes in PPS(+) cases is not due to the direct action of PPS on astrocytes.

PPS(+) cases in our study included only one case of sCJD (case 1). Although PPS infusion was started 3 months after disease onset, case 1 did not show any improvement in clinical features and the ratio of PrP^{res}/total PrP was comparable with PPS(−) sCJD cases. Meanwhile, two PPS(+) cases (cases 2 and 3) showed a relatively low ratio of PrP^{res}/total PrP. Because case 2 (dCJD) showed synaptic-type PrP deposition and type 1 PrP^{res} accumulation, it was considered to be a referential case to compare with PPS(−) CJD cases. Terada *et al.* also reported a reduction of PrP^{res} in a sCJD brain with PPS treatment.[23] In case 3 with GSS, PrP^{res} signals were very faint. It is possible that the molecular weights of plaque-type PrP deposition were too large to be detected through electrophoresis in these gels. Parchi *et al.* reported that immunoblot analysis of GSS P102L patients showed two major PrP^{res} signals with molecular masses of 21 and 8 kDa, and that the GSS patients with only the 8 kDa fragment showed mainly plaque-type PrP deposition.[24] In our study, the GSS patient with a P102L mutation showed both plaque-type PrP deposition and synaptic deposition, although Western blotting with PK treatment showed only PrP^{res} around 8 kDa. In this case, PrP^{res} might have a low resistance to PK treatment. Therefore, it may not be appropriate to compare the ratio of PrP^{res}/total PrP of case 3 to those of PPS(−) CJD cases. In case 4 with dCJD with plaque-type PrP deposits, Western blot analysis detected PrP^{res} fragments with intermediate size between types 1 and 2. Kobayashi *et al.* reported that the intermediate type PrP^{res} was seen in all examined dCJD cases with 129 methionine/methionine and plaque-type PrP deposits.[25]

Among PPS(+) cases, cases 1 and 2 showed lower indices of oligomeric PrP/total PrP than the indices of PPS(−) cases. PPS treatment might have reduced oligomeric PrP by reducing PrP^{res}. Alternatively, another study has reported that PrP fragments form amyloid aggregates in the presence of heparin which has a similar effect to PPS.[26] Therefore, oligomeric PrP in PPS(+) may be accumulated into fibrils. In our study, we did not evaluate fibrils because fibrils are difficult to electrophorese. Contrary to the reduction of oligomeric PrP/total PrP indices, monomeric PrP/total PrP indices in PPS(+) cases showed similar values to PPS(−) cases. The indices of monomeric PrP/total PrP were decreased, especially in cases with a brain weight of less than 1000 g. In these cases, PrP^{c} may have been depleted because of severe neuronal loss. Recently, oligomeric PrP was reported as the most infectious unit[17] and another study suggested that oligomeric PrP specifically inhibits the 26S proteasome, thus mediating a mechanism for intracellular neurotoxicity.[18]

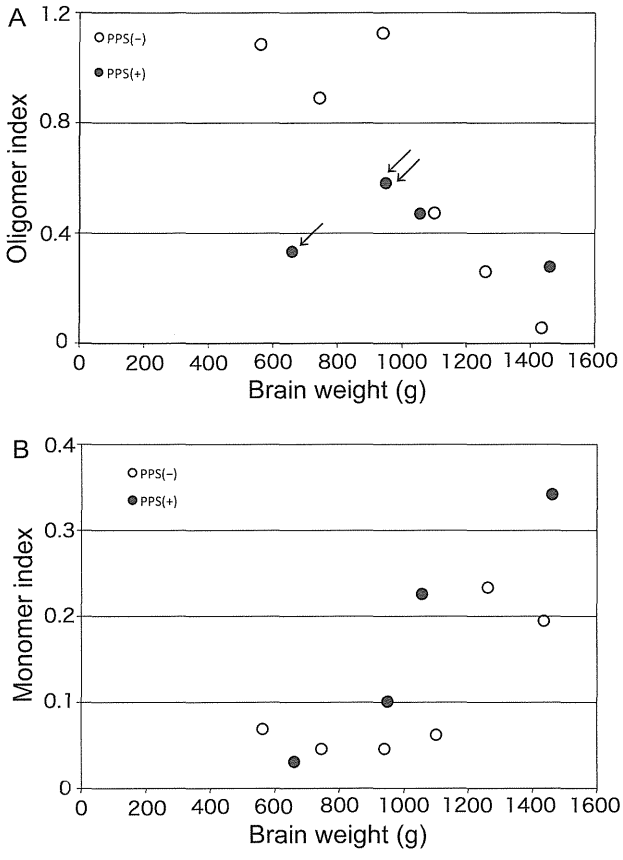

Fig. 6 Relationship between oligomeric PrP/total PrP indices and brain weight (A), or between monomeric PrP/total PrP indices and brain weight (B). (A) The oligomeric PrP/total PrP index was calculated by comparing the signals of fraction 3 to the signals of pre-column samples. In pentosan polysulfate negative (PPS(−)) cases (open circles), the oligomeric/total PrP indices are increased in accordance with brain weight loss. This tendency is also found in the PPS(+) cases (closed circles). The oligomeric PrP/total PrP indices in the PPS(+) cases are relatively low, particularly in the advanced cases with severe brain atrophy (case 1 (arrow) and case 2 (double arrows)). (B) The monomeric PrP/total PrP indices were calculated by comparing the signals of fraction 7 to the signals of pre-column samples. Monomeric PrP/total PrP indices of the advanced cases with severe brain atrophy are decreased irrespective of PPS treatment.

Doh-ura *et al.* reported that PPS infusion not only decreased PrP deposition but also reduced neurodegenerative changes in a rodent model.[9] However, in the rodent model PPS treatment could be started at the preclinical stage, whereas PPS treatment for patients was usually started at an advanced clinical stage. In the animal model, PPS treatment at an early or a late preclinical stage of the infection prolonged the incubation time by 2.4 or 1.7 times that of the control mice. Furthermore, the dosage of PPS in the animal model (460 μg/kg/day) was higher than the dosage for the human cases (120 μg/kg/day at a maximum).[9] Thus, if we could start PPS treatment at an earlier clinical stage or administer prophylactic PPS, the treatment might have beneficial effects on patients with prion diseases as shown in the experimental animal model.[9] Indeed the low indices of oligomeric PrP/total PrP were detected in two cases, but these cases showed no apparent clinicopathological improvements. Therefore, the therapeutic effects of intraventricular PPS infusion for human prion diseases are still uncertain.

ACKNOWLEDGMENTS

This work was funded by Grants-in-Aid for Scientific Research (B) (No. 22300116) and (C) (No. 21500337) from the Japan Society for the Promotion of Science (JSPS) and by the Health and Labor Sciences Research Grants (Research on Measures for Intractable Diseases) from the Ministry of Health, Labor and Welfare of Japan. The authors thank Ms Sachiko Koyama for her technical assistance. The authors also thank Drs Yoshio Tsuboi, Nobutaka Ishizu, Hiroshi Kurisaki and Shigeo Murayama for providing clinical data and pathological materials.

REFERENCES

1. Creutzfeldt HG. On a particular focal disease of the central nervous system (preliminary communication), 1920. *Alzheimer Dis Assoc Disord* 1989; **3**: 3–25.
2. Prusiner SB. Prions. *Proc Natl Acad Sci USA* 1998; **95**: 13363–13383.
3. Doh-Ura K, Iwaki T, Caughey B. Lysosomotropic agents and cysteine protease inhibitors inhibit scrapie-associated prion protein accumulation. *J Virol* 2000; **74**: 4894–4897.
4. Korth C, May BC, Cohen FE, Prusiner SB. Acridine and phenothiazine derivatives as pharmacotherapeutics for prion disease. *Proc Natl Acad Sci USA* 2001; **98**: 9836–9841.
5. Barret A, Tagliavini F, Forloni G *et al.* Evaluation of quinacrine treatment for prion diseases. *J Virol* 2003; **77**: 8462–8469.
6. Collins SJ, Lewis V, Brazier M, Hill AF, Fletcher A, Masters CL. Quinacrine does not prolong survival in a murine Creutzfeldt-Jakob disease model. *Ann Neurol* 2002; **52**: 503–506.
7. Collinge J, Gorham M, Hudson F *et al.* Safety and efficacy of quinacrine in human prion disease (PRION-1 study): a patient-preference trial. *Lancet Neurol* 2009; **8**: 334–344.
8. Caughey B, Brown K, Raymond GJ, Katzenstein GE, Thresher W. Binding of the protease-sensitive form of

PrP (prion protein) to sulfated glycosaminoglycan and congo red [corrected]. *J Virol* 1994; **68**: 2135–2141.
9. Doh-ura K, Ishikawa K, Murakami-Kubo I *et al.* Treatment of transmissible spongiform encephalopathy by intraventricular drug infusion in animal models. *J Virol* 2004; **78**: 4999–5006.
10. Caughey B, Raymond GJ. Sulfated polyanion inhibition of scrapie-associated PrP accumulation in cultured cells. *J Virol* 1993; **67**: 643–650.
11. Shyng SL, Lehmann S, Moulder KL, Harris DA. Sulfated glycans stimulate endocytosis of the cellular isoform of the prion protein, PrPC, in cultured cells. *J Biol Chem* 1995; **270**: 30221–30229.
12. Todd NV, Morrow J, Doh-ura K *et al.* Cerebroventricular infusion of pentosan polysulphate in human variant Creutzfeldt-Jakob disease. *J Infect* 2005; **50**: 394–396.
13. Rainov NG, Tsuboi Y, Krolak-Salmon P, Vighetto A, Doh-Ura K. Experimental treatments for human transmissible spongiform encephalopathies: is there a role for pentosan polysulfate? *Expert Opin Biol Ther* 2007; **7**: 713–726.
14. Tsuboi Y, Doh-Ura K, Yamada T. Continuous intraventricular infusion of pentosan polysulfate: clinical trial against prion diseases. *Neuropathology* 2009; **29**: 632–636.
15. Bone I, Belton L, Walker AS, Darbyshire J. Intraventricular pentosan polysulphate in human prion diseases: an observational study in the UK. *Eur J Neurol* 2008; **15**: 458–464.
16. Caughey B, Lansbury PT. Protofibrils, pores, fibrils, and neurodegeneration: separating the responsible protein aggregates from the innocent bystanders. *Annu Rev Neurosci* 2003; **26**: 267–298.
17. Silveira JR, Raymond GJ, Hughson AG *et al.* The most infectious prion protein particles. *Nature* 2005; **437**: 257–261.
18. Kristiansen M, Deriziotis P, Dimcheff DE *et al.* Disease-associated prion protein oligomers inhibit the 26S proteasome. *Mol Cell* 2007; **26**: 175–188.
19. Minaki H, Sasaki K, Honda H, Iwaki T. Prion protein oligomers in Creutzfeldt-Jakob disease detected by gel-filtration centrifuge columns. *Neuropathology* 2009; **29**: 536–542.
20. Lue LF, Kuo YM, Roher AE *et al.* Soluble amyloid beta peptide concentration as a predictor of synaptic change in Alzheimer's disease. *Am J Pathol* 1999; **155**: 853–862.
21. Sharon R, Bar-Joseph I, Frosch MP, Walsh DM, Hamilton JA, Selkoe DJ. The formation of highly soluble oligomers of alpha-synuclein is regulated by fatty acids and enhanced in Parkinson's disease. *Neuron* 2003; **37**: 583–595.
22. Sasaki K, Minaki H, Iwaki T. Development of oligomeric prion-protein aggregates in a mouse model of prion disease. *J Pathol* 2009; **219**: 123–130.
23. Terada T, Tsuboi Y, Obi T *et al.* Less protease-resistant PrP in a patient with sporadic CJD treated with intraventricular pentosan polysulphate. *Acta Neurol Scand* 2010; **121**: 127–130.
24. Parchi P, Chen SG, Brown P *et al.* Different patterns of truncated prion protein fragments correlate with distinct phenotypes in P102L Gerstmann-Straussler-Scheinker disease. *Proc Natl Acad Sci USA* 1998; **95**: 8322–8327.
25. Kobayashi A, Asano M, Mohri S, Kitamoto T. Cross-sequence transmission of sporadic Creutzfeldt-Jakob disease creates a new prion strain. *J Biol Chem* 2007; **282**: 30022–30028.
26. Cortijo-Arellano M, Ponce J, Durany N, Cladera J. Amyloidogenic properties of the prion protein fragment PrP(185-208): comparison with Alzheimer's peptide Abeta(1-28), influence of heparin and cell toxicity. *Biochem Biophys Res Commun* 2008; **368**: 238–242.